



Recent Advances in Micromechanics of Materials

# A phenomenological model for microstructural evolution during plastic flow

John L. Bassani<sup>a,\*</sup>, Haizhen Pan<sup>b</sup><sup>a</sup> Mechanical Engineering and Applied Mechanics, University of Pennsylvania, Philadelphia, PA 19104, USA<sup>b</sup> Holtec International, Marlton, NJ 08053, USA

## ARTICLE INFO

## Article history:

Available online 13 April 2012

## Keywords:

Orthotropic plastic flow

Plastic spin

Microstructural evolution

## ABSTRACT

A class of materials is considered that possesses local orthotropic symmetries. Constitutive models with microstructural evolution are developed within a conventional elastic–plastic multiplicative decomposition. In the current configuration, the orthotropic vectors evolve with the microstructural spin, which is the difference between the material and plastic spins. Representations for tensor-valued functions for orthotropic material behavior due to Zheng (1994) are extended to develop constitutive equations for the plastic parts of the rate of stretching and the spin. A key relation is established between components of the plastic part of the rate of stretching and the plastic spin. Comparisons with experiments are promising.

© 2012 Académie des sciences. Published by Elsevier Masson SAS. All rights reserved.

## 1. Introduction

Large inelastic strains arising in deformation processing of metallic alloys, metal–matrix composites, polymers, or polymer matrix composites as well as in mechanisms of ductile failure typically involve significant changes in microstructure. Length scales involved range from submicron to millimeters as dislocation cell structures, grain shapes, particle or fiber distributions, polycrystalline texture, and/or molecular orientation, etc., evolve. In general, non-random microstructures impart anisotropic macroscopic properties. For example, orthotropic yield functions have been used to predict forming limits in textured polycrystalline metals when bi-axial strain states are aligned with principle axes of anisotropy, in which case the symmetries of the microstructure are fixed during deformation. Comparable predictions based upon phenomenological models do not exist for off-axis forming limits. One prominent application of the latter is plastic forming of polycrystalline sheet metal into a complex shape. For such problems involving non-uniform deformations at macroscopic scales, predictions that account for microstructural evolution for the most part require elaborate micromechanical material models and extensive computations. Indeed, simple but reasonably accurate phenomenological models are lacking that account for microstructural evolution at the same level of phenomenology as flow rules for plastic strains. The development of such models is the subject of this paper, which builds upon work of Dafalias [1–3].

Over the last 30 years, there has been substantial progress in modeling large-strain plastic deformation, and no attempt is made here to review that development. The reader is referred to two recent treatises [4,5], which include phenomenological engineering plasticity theories and micromechanical models such as those that have been a hallmark of A. Zaoui's many contributions [6–8].

To characterize the overall effect of microstructural evolution at the continuum level, we assume that the anisotropy can be characterized by three mutually orthogonal symmetry planes. Furthermore, orthotropic symmetry is assumed to persist

\* Corresponding author.

E-mail address: [bassani@seas.upenn.edu](mailto:bassani@seas.upenn.edu) (J.L. Bassani).

at each material point throughout deformation, while the orientation of the orthotropic triad – director vectors in the sense of Mandel [9,10] – in general varies spatially throughout a non-uniformly deformed sample. Elastic–plastic constitutive equations are developed that include the spin of those axes (an anti-symmetric, second-order tensor) and specification of material properties in those directions. Within a standard elastic–plastic multiplicative decomposition, the intermediate configuration is assumed to be isoclinic in the sense that the director vectors retain the same orientation as in the reference configuration. Furthermore, we define the microstructural spin to be the difference between the material and plastic spins. Consequently, to fully characterize microstructural evolution, constitutive relations are required for the plastic parts of the rate of stretching and the spin, which is the central topic in this paper. One proposal was to derive the plastic part of the velocity gradient, which includes plastic spin, from potential functions (i.e., normality relations), but no explicit functions were given [11,12]. Dafalias [1–3] and Loret [13] utilized representation theory for tensors to formulate equations for the plastic part of spin in the current configuration. Those investigations had limited success in describing observed behaviors.

Indeed, experiments have established the fact that microstructural spin is generally distinct from the material spin, i.e. plastic spin does not vanish. Nevertheless, from a thermodynamic perspective, Van der Giessen [14,15] noted that a constitutive equation for plastic spin written in current configuration variables does not directly associate energy dissipation with microstructural evolution. In this work, constitutive equations for plastic spin are derived in the intermediate configuration and admit such energy dissipation. Representations for scalar-valued and tensor-valued functions [16] expressed in terms of tensors in that configuration are utilized to develop a key relation between the plastic parts of deformation rate and spin in the intermediate configuration. Predictions that follow are shown to agree well with available experimental studies that measured the rotation of orthotropic axes (preferred directions) in textured polycrystals.

Standard notation is used throughout. Boldface symbols are tensors,  $\text{tr}\mathbf{A}$  is the trace of the second-order tensor  $\mathbf{A}$ , superscript  $T$  denotes transpose, subscripts  $s$  and  $a$  denote symmetric and anti-symmetric parts of a tensor, respectively, superscripts  $e$  and  $p$  denote the elastic and plastic parts, respectively, subscript  $I$  denotes the intermediate configuration, and a superposed dot denotes the material time derivative. Tensor components are written with respect to Cartesian coordinate systems and products are defined in as:  $(\mathbf{a} \otimes \mathbf{b})_{ij} = a_i b_j$ ,  $(\mathbf{AB})_{ij} = A_{ik} B_{kj}$ , and  $\mathbf{A} : \mathbf{B} = A_{ij} B_{ij}$ . The symmetric unit second-order tensor  $\mathbf{I}$  has components  $\delta_{ij}$ , the Kronecker delta.

## 2. Framework for the phenomenological model

The evolution of microstructure, e.g. polycrystalline texture, particle distributions, or molecular orientation, affects anisotropic macroscopic response. For example, initially random (isotropic) textures evolve through large-strain processes to impart continuously-varying preferred orientations. As a result, wire drawing leads to transversely isotropic properties and sheet rolling leads to orthotropic properties. As a sheet is deformed into a complex shape, texture continues to evolve but inevitably will be non-uniform throughout the part. For deformation-induced anisotropy, it is plausible to assume that the *local anisotropy possesses three mutually orthogonal symmetry planes* at each material point. This approximation, which we refer to as persistent orthotropic symmetry, is adopted. The principle axes of anisotropy (director vectors) are orthotropic unit vectors, denoted  $\hat{\mathbf{e}}_i$ ,  $i = 1, 3$ , that rotate as the material deforms and characterize the effective symmetries of the microstructure, which spatially vary throughout a non-uniformly deformed sample.

The *intermediate configuration* is taken to be *isoclinic* within a multiplicative elastic–plastic decomposition of the deformation gradient (a standard assumption in the finite-strain theory of crystal plasticity [4,5]). Rotation of the orthotropic triad is determined by the *microstructural spin*, which is an anti-symmetric tensor that is taken to be the difference between the material and plastic spins [9–12]. Consequently, to fully characterize microstructural evolution, constitutive relations are required for the plastic parts of the rate of stretching and the spin. Dafalias [1–3] and Loret [13] utilized representation theory for tensors to formulate equations for the plastic part of spin in the current configuration. In what follows, we develop constitutive equations for plastic spin in the intermediate configuration, which is associated with plastic dissipation. Those equations are based upon representations for scalar-valued and tensor-valued functions [16–18]. The latter imply *key relations between the plastic parts of the deformation rate and the spin in the intermediate configuration* which are exact and lead to a relatively simple characterization of microstructural evolution.

### 2.1. Kinematics of microstructural evolution

The deformation gradient,  $\mathbf{F}$ , maps the neighborhood of a material point in the initial (reference) configuration ( $B_0$ ) to a point in the current configuration ( $B$ ). Let  $\hat{\mathbf{e}}_{0i}$  and  $\hat{\mathbf{e}}_i$  ( $i = 1, 3$ ) denote orthonormal vectors at each material point that characterize the orthotropic material symmetries in the configurations  $B_0$  and  $B$ , respectively. In the setting of finite elastic–plastic deformations, the multiplicative decomposition  $\mathbf{F} = \mathbf{F}^e \mathbf{F}^p$  is adopted [4,5]. The intermediate “configuration” ( $B_I$ ) is the mapping of the initial configuration by the plastic part of the deformation gradient,  $\mathbf{F}^p$ , and the director vectors have orientation  $\hat{\mathbf{e}}_{0i}$  in that isoclinic configuration. The velocity gradient,  $\mathbf{L} = \dot{\mathbf{F}}\mathbf{F}^{-1}$  is partitioned into elastic and plastic parts as are its symmetric and anti-symmetric parts, i.e. the rate of stretching ( $\mathbf{D}$ ) and spin ( $\mathbf{W}$ ) tensors:

$$\mathbf{L} = \mathbf{L}^e + \mathbf{L}^p \quad (1)$$

where

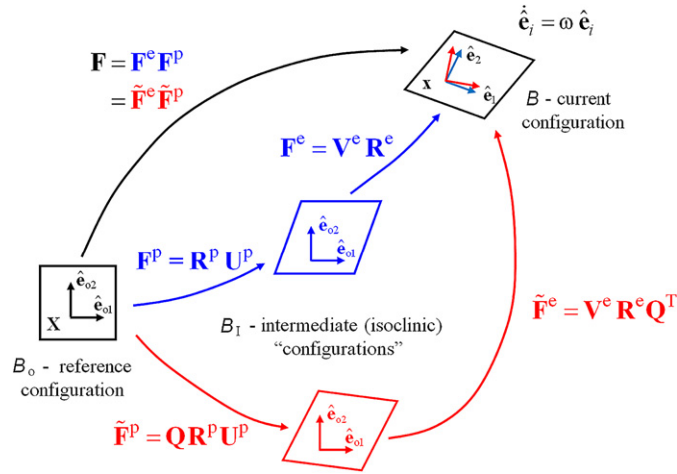


**Fig. 1.** The orientation of the orthonormal director vectors in the current configuration determines the partition of rigid rotation associated with  $F^e$  and  $F^P$ , which in turn specifies the intermediate configuration.

$$L^e \equiv \dot{F}^e F^{e-1} \quad \text{and} \quad L^P \equiv F^e \dot{F}^P F^{P-1} F^{e-1} \equiv F^e L_1^P F^{e-1} \tag{2}$$

and

$$D = (L)_s = D^e + D^P \quad \text{and} \quad W = (L)_a = W^e + W^P \tag{3}$$

The plastic part of the velocity gradient in the intermediate configuration is denoted  $L_1^P$ , and

$$D_1^P = (\dot{F}^P F^{P-1})_s \quad \text{and} \quad W_1^P = (\dot{F}^P F^{P-1})_a \tag{4}$$

Since the microstructural vectors are assumed to remain orthonormal at every stage of deformation (i.e., in the current configuration), their evolution can be expressed in rate form in terms of the anti-symmetric tensor  $\omega$  that governs the spin of the microstructure:

$$\dot{\hat{e}}_i = \omega \hat{e}_i, \quad i = 1, 3, \quad \text{where } \omega = W^e = (\dot{F}^e F^{e-1})_a \tag{5}$$

Since  $W^e = W - W^P$ , with  $W$  given, a constitutive relation for plastic spin determines the evolution of the vectors that characterize the local anisotropy at each material point. Among many possibilities, this choice for the evolution of the director vectors is simple in the sense that it preserves orthotropic symmetries and, as we shall see, leads to accurate predictions of macroscopic observations that also assume persistent orthotropy. Nevertheless, other choices can readily be considered if experimental data dictates the need (see [19] for a related discussion of the evolution of slip vectors in the context of single crystals).

Since spin is an anti-symmetric second-order tensor, there are 3 constitutive functions to be prescribed. That the intermediate configuration is only determined to within an arbitrary rotation can be seen from the following argument. Let  $F = V^e R U^P$ , where  $R$  is a rotation (proper orthogonal tensor) and  $V^e$  and  $U^P$  are stretch tensors associated with polar decompositions of  $F^e$  and  $F^P$ . The decomposition  $R = R^e R^P$  is not unique, since  $F = F^e F^P = \tilde{F}^e \tilde{F}^P$  where  $\tilde{F}^P = Q R^P U^P$  and  $\tilde{F}^e = V^e R^e Q^T$  with  $Q$  denoting an arbitrary rotation, which is depicted in the diagram of Fig. 1. This illustrates the facts that: i) the intermediate configuration is not uniquely determined by the multiplicative decomposition, while ii) the orientation of the director vectors in the current configuration serves to uniquely determine the plastic part of the rotation,  $R^P$  and, therefore, also  $R^e$ .

In simulations of texture evolution under shear deformation, Tugcu and Neale [20] assumed that the orthotropic axes rotate with the orthogonal tensor associated with rigid-body motion. That simple model, as well as the constitutive models for plastic spin in the work of Dafalias [1–3,21], cannot adequately describe experiments such as those cited below. In contrast, predictions based upon (5) with the constitutive equations for plastic spin outlined below do rather well in accounting for measured rotation of the orthotropic axes in textured sheet materials, even when only using Hill's quadratic yield function [22] for orthotropic materials as presented in Section 3.

## 2.2. Stress measures

In principle, constitutive relations can be defined in any one of the three configurations and appropriately transformed to another as needed. In this work, plastic behavior is assumed to possess persistent orthotropic symmetry, and the isoclinic intermediate configuration  $B_1$  is most convenient.

Various work-conjugate variables are defined in the intermediate (isoclinic) configuration from the rate of stress working per unit reference volume:

$$\dot{W} = \boldsymbol{\tau} : \mathbf{D} = \mathbf{S}^e : \dot{\mathbf{E}}^e + \boldsymbol{\Sigma}_I : \mathbf{L}_I^P = \dot{W}^e + \dot{W}^P \quad (6)$$

where  $\boldsymbol{\tau} = \boldsymbol{\tau}^T$  is the Kirchhoff stress,  $\mathbf{S}^e = \mathbf{F}^{e-1} \boldsymbol{\tau} \mathbf{F}^{e-T}$ ,  $\dot{\mathbf{E}}^e = \frac{1}{2}(\mathbf{F}^{eT} \dot{\mathbf{F}}^e - \mathbf{I})$ , and the generally non-symmetric intermediate configuration stress [9,12,14]:

$$\boldsymbol{\Sigma}_I = \mathbf{F}^{eT} \boldsymbol{\tau} \mathbf{F}^{e-T} = \boldsymbol{\Sigma}_{Is} + \boldsymbol{\Sigma}_{Ia} \quad (7)$$

From (6) with (4) and (7), the rate of energy dissipation can be written as:

$$\dot{W}^P = \boldsymbol{\tau} : \mathbf{D}^P = \boldsymbol{\Sigma}_I : \mathbf{L}_I^P = \boldsymbol{\Sigma}_{Is} : \mathbf{D}_I^P + \boldsymbol{\Sigma}_{Ia} : \mathbf{W}_I^P \quad (8)$$

i.e.,  $\boldsymbol{\Sigma}_{Is}$  and  $\boldsymbol{\Sigma}_{Ia}$  are conjugate to  $\mathbf{D}_I^P$  and  $\mathbf{W}_I^P$ , respectively. Even if  $\boldsymbol{\Sigma}_{Ia}$  is zero or very small, plastic spin will implicitly contribute to dissipation since it affects  $\mathbf{D}^P$  and  $\mathbf{D}_I^P$  through evolution of the orthotropic material axes. Furthermore, an explicit contribution to  $\dot{W}^P$  is not necessary to establish a constitutive equation for  $\mathbf{W}_I^P$ . If the material is elastically isotropic, then  $\boldsymbol{\Sigma}_{Ia} = \mathbf{0}$  [10]. More generally, if the elastic strain is small, i.e.,  $\mathbf{V}^e = \mathbf{I} + \varepsilon \bar{\mathbf{V}}$  with  $|\varepsilon| \ll 1$ , then  $\boldsymbol{\Sigma}_{Is} = \mathbf{R}^{eT} \boldsymbol{\tau} \mathbf{R}^e + \mathcal{O}(\varepsilon^2 \boldsymbol{\tau})$  and  $\boldsymbol{\Sigma}_{Ia} = \mathcal{O}(\varepsilon \boldsymbol{\Sigma}_{Is})$ . Therefore, even for anisotropic elasticity,  $\boldsymbol{\Sigma}_{Ia}$  is small compared with  $\boldsymbol{\Sigma}_{Is}$  if elastic strain is small.

### 2.3. Representations for orthotropic plastic behavior

Representation theory for tensor-valued functions of tensors, which was introduced in continuum mechanics by Rivlin and Ericksen [23] (followed by many others over a 40 year period; see, e.g., [24–27]), is utilized to construct constitutive equations for plastic spin in the intermediate configuration. Here, we build on the more recent results of Zheng in [16], which includes an extensive bibliography to the earlier works. For orthotropic behavior, one generally thinks of employing two symmetric rank-one orientation tensors,  $\hat{\mathbf{A}}_{o1} = \hat{\mathbf{e}}_{o1} \otimes \hat{\mathbf{e}}_{o1}$  and  $\hat{\mathbf{A}}_{o2} = \hat{\mathbf{e}}_{o2} \otimes \hat{\mathbf{e}}_{o2}$ , with the third derived from orthogonality, but in fact as Zheng [16] has shown that only one orientation tensor is required:

$$\hat{\mathbf{M}}_0 = \hat{\mathbf{A}}_{o1} - \hat{\mathbf{A}}_{o2} \quad \text{with} \quad \hat{\mathbf{M}}_0^2 = \hat{\mathbf{A}}_{o1} + \hat{\mathbf{A}}_{o2} \quad (9)$$

Therefore, we will investigate constitutive representations for  $\mathbf{D}_I^P$  and  $\mathbf{W}_I^P$  in terms of  $\boldsymbol{\Sigma}_I$  and  $\hat{\mathbf{M}}_0$ .

Representations for invariants and generators of orthotropic tensor functions are given in Zheng [16]. From the expressions for invariants in terms of components of tensors in the  $\hat{\mathbf{e}}_{oi}$  bases, Pan and Bassani [28] have shown rigorously that further reductions, so-called syzygies, are possible. They show that complete functional set of 13 invariants of  $\boldsymbol{\Sigma}_I$  and  $\hat{\mathbf{M}}_0$  are:

$$\{I_\kappa, \kappa = 1, 13\} = \{\text{tr}(\boldsymbol{\Sigma}_{Is}), \text{tr}(\hat{\mathbf{M}}_0 \boldsymbol{\Sigma}_{Is}), \text{tr}(\hat{\mathbf{M}}_0^2 \boldsymbol{\Sigma}_{Is}), \text{tr}(\boldsymbol{\Sigma}_{Is}^2), \text{tr}(\hat{\mathbf{M}}_0 \boldsymbol{\Sigma}_{Is}^2), \text{tr}(\hat{\mathbf{M}}_0^2 \boldsymbol{\Sigma}_{Is}^2), \\ \text{tr}(\boldsymbol{\Sigma}_{Ia}^2), \text{tr}(\hat{\mathbf{M}}_0 \boldsymbol{\Sigma}_{Ia}^2), \text{tr}(\hat{\mathbf{M}}_0^2 \boldsymbol{\Sigma}_{Ia}^2), \text{tr}(\hat{\mathbf{M}}_0 \boldsymbol{\Sigma}_{Is} \boldsymbol{\Sigma}_{Ia}), \text{tr}(\hat{\mathbf{M}}_0^2 \boldsymbol{\Sigma}_{Is} \boldsymbol{\Sigma}_{Ia}), \text{tr}(\boldsymbol{\Sigma}_{Is}^3), \text{tr}(\hat{\mathbf{M}}_0^2 \boldsymbol{\Sigma}_{Ia}^2 \hat{\mathbf{M}}_0 \boldsymbol{\Sigma}_{Ia})\} \quad (10)$$

For example, for orthotropic behavior, the yield function  $F$  expressed in the intermediate configuration can depend only on the invariants given in (10), i.e.,  $F = F(\{I_\kappa\})$ .

Pan and Bassani [28] also have derived reduced sets of orthotropic generators for second-order tensors. The symmetric, second-order tensor-valued function  $\mathbf{D}_I^P$  is composed from 6 symmetric generators:

$$\mathbf{D}_I^P = \alpha_1 \mathbf{I} + \alpha_2 \hat{\mathbf{M}}_0 + \alpha_3 \hat{\mathbf{M}}_0^2 + \alpha_4 \boldsymbol{\Sigma}_{Is} + \alpha_5 (\hat{\mathbf{M}}_0 \boldsymbol{\Sigma}_{Is} + \boldsymbol{\Sigma}_{Is} \hat{\mathbf{M}}_0) + \alpha_6 (\hat{\mathbf{M}}_0^2 \boldsymbol{\Sigma}_{Is} + \boldsymbol{\Sigma}_{Is} \hat{\mathbf{M}}_0^2) \quad (11)$$

where  $\mathbf{I}$  is the second-order identity tensor and  $\alpha_\mu$ 's are scalar-valued functions of the invariants  $\{I_\kappa\}$ . The anti-symmetric, second-order tensor-valued function  $\mathbf{W}_I^P$  is composed of 3 anti-symmetric generators:

$$\mathbf{W}_I^P = \beta_1 (\hat{\mathbf{M}}_0 \boldsymbol{\Sigma}_s - \boldsymbol{\Sigma}_s \hat{\mathbf{M}}_0) + \beta_2 (\hat{\mathbf{M}}_0^2 \boldsymbol{\Sigma}_s - \boldsymbol{\Sigma}_s \hat{\mathbf{M}}_0^2) + \beta_3 (\hat{\mathbf{M}}_0 \boldsymbol{\Sigma}_s \hat{\mathbf{M}}_0^2 - \hat{\mathbf{M}}_0^2 \boldsymbol{\Sigma}_s \hat{\mathbf{M}}_0) \quad (12)$$

where the coefficients  $\beta_\nu$ 's depend on the invariants  $\{I_\kappa\}$ . Note that  $\boldsymbol{\Sigma}_{Ia}$  only enters  $\mathbf{D}_I^P$  and  $\mathbf{W}_I^P$  through the coefficients  $\alpha_\mu$  in (11) and  $\beta_\nu$  in (12), respectively. For isotropic response, plastic spin (12) vanishes, which is consistent with the fact that random microstructures lack preferred directions. The results above for generators that depend linearly on  $\boldsymbol{\Sigma}_{Is}$  encompass most, if not all, classical flow theories for orthotropic plastic behavior.

### 2.4. Constitutive equations for plastic spin

From (11) and (12), one can show that  $\mathbf{W}_I^P$  is directly related to the shear components of  $\mathbf{D}_I^P$  expressed in terms of components with respect to the bases  $\hat{\mathbf{e}}_{oi}$  which define the orthotropic symmetry [28]:

$$\hat{W}_{112}^P = \eta_3 \hat{D}_{112}^P, \quad \hat{W}_{113}^P = \eta_2 \hat{D}_{113}^P, \quad \hat{W}_{123}^P = \eta_1 \hat{D}_{123}^P \quad (13)$$

where  $\eta_i(\{I_\kappa\})$  are scalar-valued functions depending on the invariants and the overstrike  $\hat{\cdot}$  denotes components with respect to the orthotropic bases  $\hat{\mathbf{e}}_{oi}$ . Therefore, the plastic part of spin in the intermediate configuration  $\mathbf{B}_1$  depends upon the non-coaxiality between  $\mathbf{D}_1^p$  and the initial orthotropic axes  $\hat{\mathbf{e}}_{oi}$ , which intuitively makes sense. Furthermore, if the shear components of  $\hat{D}_{ij}^p$  vanish, then  $\mathbf{W}_1^p = 0$  and, from (2)–(5),  $\boldsymbol{\omega} = \mathbf{W}$ .

The key relations (13), which imply *persistent orthotropic material symmetry*, are exact (since they have been derived from representation theory) and reflect the *non-coaxiality in the intermediate configuration of the plastic part of the rate of stretching and the orthonormal director vectors*. These relations form the basis of constitutive equations for microstructural evolution, i.e. the evolution of material symmetries. The  $\eta_i$  are functions of the invariants (10) of  $\boldsymbol{\Sigma}_1$  and  $\hat{\mathbf{M}}_0$ , must be homogeneous of degree zero in stress, and will depend upon the material and its initial texture. We could construct forms for  $\eta_i$  from polynomials in ratios of the  $I_\kappa$ 's that are homogeneous of degree zero. An alternative strategy, which is pursued below, begins from the notion of non-coaxiality; cf. discussion following (13). We note that  $\hat{\Sigma}_{1s11}$ ,  $\hat{\Sigma}_{1s22}$  and  $\hat{\Sigma}_{1s33}$  can be expressed in terms of  $I_1$ ,  $I_2$  and  $I_3$  from the set of invariants (10). Therefore, from (11), we readily see that  $\hat{D}_{111}^p$ ,  $\hat{D}_{122}^p$  and  $\hat{D}_{133}^p$  are also scalar-valued functions of those invariants. In general, only the squares of the shear components of  $\mathbf{D}_1^p$ , and not the shear components themselves, are functions of the invariants.

Our attempts to correlate certain observations of textured evolution for polycrystalline metals have guided forms for  $\eta_i$  proposed below. Consider tensile loading in the plane  $\mathbf{e}_1$ – $\mathbf{e}_2$  of an orthotropic sheet; that plane coincides with the  $\hat{\mathbf{e}}_1$ – $\hat{\mathbf{e}}_2$  orthotropic symmetry plane, where  $\beta$  is the angle between  $\mathbf{e}_1$  and  $\hat{\mathbf{e}}_1$  (see Fig. 1). A common observation is that the sense of rotation of  $\hat{\mathbf{e}}_1$  towards or away from the tensile axis ( $\mathbf{e}_1$ ) depends upon the initial orientation of the tensile axis [29–34]. In particular, the sense of rotation depends upon whether the initial angle  $\beta_o$  is greater or less than a critical angle, which approximately equals 45°. That fact implies that  $\eta_i$  cannot be constant. The microstructural spin is zero at that critical angle, where  $\hat{D}_{112}^p$  reaches an extreme value, and  $\hat{D}_{111}^p - \hat{D}_{122}^p$  is zero. Initially, we will consider  $\eta_i$ 's to depend only on diagonal components of  $\mathbf{D}_1^p$  with, for example,  $\eta_3$  reducing to a constant if  $\hat{D}_{111}^p = \hat{D}_{122}^p$  in planar loading. In simple shear loading, Nesterova et al. [31] observed that in the rigid-plastic limit, i.e. without elastic straining, microstructural evolution returns to its initial state when the applied shear deformation is removed. The latter suggests that the  $\eta_i$ 's are even functions of the components  $\hat{D}_{ij}^p$ . This leads to the following proposal:

$$\begin{aligned} \eta_1 &= \eta_{o1} + \frac{\xi_1}{\dot{\epsilon}_e^2} \hat{D}_{111}^p (\hat{D}_{133}^p - \hat{D}_{122}^p) \\ \eta_2 &= \eta_{o2} + \frac{\xi_2}{\dot{\epsilon}_e^2} \hat{D}_{122}^p (\hat{D}_{111}^p - \hat{D}_{133}^p) \\ \eta_3 &= \eta_{o3} + \frac{\xi_3}{\dot{\epsilon}_e^2} \hat{D}_{133}^p (\hat{D}_{122}^p - \hat{D}_{111}^p) \end{aligned} \tag{14}$$

where the six parameters  $\eta_{oi}$  and  $\xi_i$  are material constants and  $\dot{\epsilon}_e^p$  is the equivalent plastic strain rate. For example, under loading in the  $\hat{\mathbf{e}}_1$ – $\hat{\mathbf{e}}_2$  plane (considered below), from (13) and (14), the non-zero component of  $\mathbf{W}_1^p$  can be expressed in terms of on two material parameters,  $\eta_{o3}$  and  $\xi_3$ , as:

$$\hat{W}_{112}^p = \left[ \eta_{o3} + \frac{\xi_3}{\dot{\epsilon}_e^2} \hat{D}_{133}^p (\hat{D}_{122}^p - \hat{D}_{111}^p) \right] \hat{D}_{112}^p = \left[ \eta_{o3} + \frac{\xi_3}{\dot{\epsilon}_e^2} (\hat{D}_{111}^2 - \hat{D}_{122}^2) \right] \hat{D}_{112}^p \tag{15}$$

where plastic incompressibility,  $\hat{D}_{iii}^p = 0$ , leads to the second of (15).

To specify the plastic rate of stretching, we consider a normality flow rule in the intermediate configuration, i.e.,

$$\mathbf{D}_1^p = \dot{\epsilon}_e^p \frac{\partial F}{\partial \boldsymbol{\Sigma}_{1s}} = \dot{\epsilon}_e^p \mathbf{N}_1^p \tag{16}$$

For a particular choice of yield/flow function, (16) can be rewritten in terms of components of stress, and an example follows. Towards that end, consider a material in which  $\boldsymbol{\Sigma}_{1a}$  is small compared to  $\boldsymbol{\Sigma}_{1s}$ , e.g. for finite elastic–plastic deformations of metal polycrystals as discussed above. In this case, it is reasonable to assume the yield function and flow potential for  $\mathbf{D}_1^p$  only depends on  $\boldsymbol{\Sigma}_{1s}$ . This includes Hill's quadratic orthotropic yield function [22] as well as the yield functions developed by Hill [22,35,36], Bassani [37], Barlat and Lian [38], Ferron et al. [39], and many others. All of these can be written in the form:

$$F \equiv F(\hat{\Sigma}_{1s11}, \hat{\Sigma}_{1s22}, \hat{\Sigma}_{1s33}, \hat{\Sigma}_{1s23}^2, \hat{\Sigma}_{1s13}^2, \hat{\Sigma}_{1s12}^2, \hat{\Sigma}_{1s23} \hat{\Sigma}_{1s13} \hat{\Sigma}_{1s12}) \tag{17}$$

Furthermore, the yield/flow function (17) also can be expressed in terms of the seven invariants that only depend on  $\boldsymbol{\Sigma}_{1s}$ , i.e.,  $I_\kappa$ ,  $\kappa = 1$ –6 and 12.

For Hill's quadratic yield function [22], which is adopted for comparisons with experimental observations of texture evolution presented below,

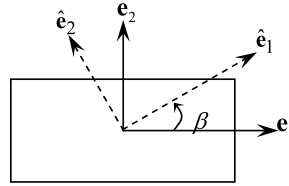


Fig. 2. Angle  $\beta$  between loading axes ( $\mathbf{e}_1$ – $\mathbf{e}_2$ ) and principle axes of anisotropy ( $\hat{\mathbf{e}}_1$ – $\hat{\mathbf{e}}_2$ ).

$$\sigma_e = \frac{1}{\sqrt{2}} [c_1(\hat{\Sigma}_{1s22} - \hat{\Sigma}_{1s33})^2 + c_2(\hat{\Sigma}_{1s33} - \hat{\Sigma}_{1s11})^2 + c_3(\hat{\Sigma}_{1s11} - \hat{\Sigma}_{1s22})^2 + 6c_4\hat{\Sigma}_{1s23}^2 + 6c_5\hat{\Sigma}_{1s13}^2 + 6c_6\hat{\Sigma}_{1s12}^2]^{1/2} \quad (18)$$

where  $\sigma_e \equiv F$  denotes the effective stress and  $c_i$ 's are parameters defining the yield anisotropy. Yield corresponds to  $\sigma_e = \sigma_Y = \text{constant}$ . Since  $F$  is homogeneous of degree one in stress, the  $\hat{N}_{ij}^p$ 's are degree zero and, from (14), (16) and (18), for example,

$$\eta_3 = \eta_{03} + \frac{\xi_3}{\sigma_e^2} (c_1 + c_2 + c_3)(\hat{\Sigma}_{1s22} - \hat{\Sigma}_{1s11})[(c_1 + c_2)\hat{\Sigma}_{1s33} - c_1\hat{\Sigma}_{1s11} - c_2\hat{\Sigma}_{1s22}] \quad (19)$$

With the flow rule relations (16), plastic spin is determined from (13) and the microstructural spin from (5). In addition to the parameters entering the yield function, e.g. the  $c_i$ 's in (18), the phenomenological relations for plastic spin involve six parameters in 3D. For in-plane loading, only 2 parameters,  $\eta_{03}$ ,  $\xi_3$ , in addition to the 3 yield parameters,  $c_1$ ,  $c_2$ ,  $c_3$ , need to be specified. In the next section, predictions for the rotation of the anisotropic axes relative to loading axes are shown to accurately reproduce experimental observations for textured polycrystals. This methodology is readily adopted for other yield functions.

### 3. Comparisons with experiments

The constitutive parameters defining orthotropic yield, flow and microstructural evolution can be fit to experimental data for texture evolution in polycrystalline metals. Consider a rolled sheet with orthonormal vectors  $\{\hat{\mathbf{e}}_{oi}\}$  characterizing the initially anisotropic symmetries, and consider planar loading in the  $\hat{\mathbf{e}}_1$ – $\hat{\mathbf{e}}_2$  plane with in-plane stressing defined with respect to the  $\mathbf{e}_1$  and  $\mathbf{e}_2$  loading axes, where  $\mathbf{e}_3 = \hat{\mathbf{e}}_3$ . Therefore, for materials with orthotropic symmetry,  $\tau_{13} = \tau_{23} = 0$ ,  $D_{13} = D_{23} = 0$ , and also  $W_{23} = -W_{32} = W_{13} = -W_{31} = 0$ , where here the components with respect to the loading axes  $\mathbf{e}_i$ . The rotation of the  $\hat{\mathbf{e}}_1$ – $\hat{\mathbf{e}}_2$  axes is about the  $\mathbf{e}_3$  ( $=\hat{\mathbf{e}}_{o3}$ ) axis is characterized by the angle  $\beta = \cos^{-1}(\mathbf{e}_1 \cdot \hat{\mathbf{e}}_1)$  (see Fig. 2). For brevity, in what follows we neglect elastic strains, which tend to be much smaller than the total strains arising in all the experiments to be considered; that is,  $\mathbf{F}^e = \mathbf{R}^e$ .

Let  $\hat{\mathbf{e}}_1 = \cos \beta \mathbf{e}_1 + \sin \beta \mathbf{e}_2$ . From (5),  $\dot{\hat{\mathbf{e}}}_1 = \boldsymbol{\omega} \hat{\mathbf{e}}_1$ , and it follows that the rate of rotation the loading axes with respect to the current orientation of the principle axis of anisotropy,  $\hat{\mathbf{e}}_1$ , is

$$\dot{\beta} = -\omega_{12} = W_{12}^p - W_{12} \quad (20)$$

For small elastic strains,  $W_{12}^p \approx W_{12}^p$  and (20) can be approximated as  $\dot{\beta} \approx \hat{W}_{12}^p - W_{12}$ . Therefore, given a constitutive equation for  $\mathbf{D}_1^p$ , from (13) with (14), only two constants  $\eta_{03}$  and  $\xi_3$  need to be specified to describe the microstructural evolution under planar loading. Note, if  $\hat{W}_{12}^p = 0$ , then the orthotropic axes spin with the material, i.e.,  $\dot{\beta} = -W_{12}$ .

The degree of anisotropy for in-plane loading requires the specification of three material parameters for two-dimensional states of stress. These are conveniently expressed in terms of:

$$s_1 = \hat{\Sigma}_2 / \hat{\Sigma}_1, \quad s_2 = \hat{\Sigma}_b / \hat{\Sigma}_1, \quad s_3 = \hat{\Sigma}_{y12} / \hat{\Sigma}_1 \quad (21)$$

where  $\hat{\Sigma}_1$  and  $\hat{\Sigma}_2$  are the uniaxial yield stresses in the  $\hat{\mathbf{e}}_{o1}$  and  $\hat{\mathbf{e}}_{o2}$  directions, respectively,  $\hat{\Sigma}_b = -\hat{\Sigma}_{1s11} = -\hat{\Sigma}_{1s22}$  is the equal bi-axial yield stress,  $\hat{\Sigma}_{y12}$  is the yield stress in shear. For isotropic behavior,  $s_1 = s_2 = 1$  and, from the von Mises criterion,  $s_3 = 0.577$ . Representative values of  $\eta_{03}$ ,  $\xi_3$ ,  $s_1$ ,  $s_2$ ,  $s_3$  for three materials from fits to experiments discussed below are given in Table 1.

For off-axis tensile and shear loading in the plane of anisotropic sheet materials, the orientation of the loading axes ( $\mathbf{e}_i$ ) relative to the principle axes of anisotropy ( $\hat{\mathbf{e}}_i$ ) tends to continuously change due to microstructural evolution (Fig. 2). Under uniaxial tensile loading, Boehler and Koss [29] and Losilla et al. [30] tested a cold-rolled steel sheet (material A) at initial angles of the tensile axes relative to the principle planes of anisotropy of  $\beta_0 = 30^\circ, 45^\circ, 60^\circ$ . The measured change in that angle as a function of the tensile strain is plotted in Fig. 3. Clearly, significant changes are seen with strains only on the order of 0.1. The tensile axes tend to rotate towards the rolling direction in the first two cases and towards the transverse direction in the third case. The solid curves in Fig. 3 are predictions based upon the phenomenological relations (15). Neglecting

**Table 1**

Parameters entering the equation for plastic spin (15) and the yield function (18) with (21) for three materials fit to experimental data.

Material	$\eta_{03}$	$\xi_3$	$s_1$	$s_2$	$s_3$
A	1.5	30.0	1.06	1.06	0.59
B	-1.0	80.0	1.03	0.98	0.80
C	-2.0	80.0	0.96	1.01	0.67

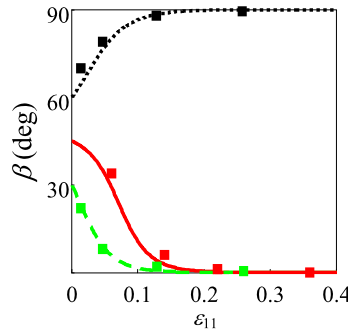


**Fig. 3.** Rotation of the uniaxial tensile axis relative to the principle axis of anisotropy in a steel sheet as a function of strain for initial orientations  $\beta_0 = 30^\circ, 45^\circ,$  and  $60^\circ$ . Data (squares) are from Boehler and co-workers [29,30] and curves are our predictions for material A.

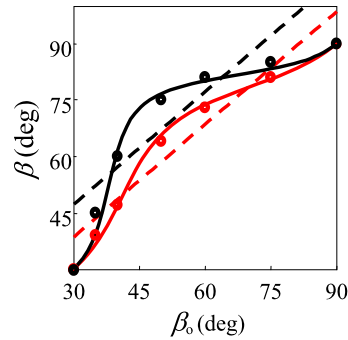


**Fig. 4.** Rotation of the axes of shear loading relative to the principle axes of anisotropy in a steel sheet following shear strains of  $\gamma = -0.3$  (red) and  $-0.6$  (black). Data (dots) are from Nesterova et al. [31]. Predictions from the proposed phenomenological model for material B are solid curves and those for vanishing plastic spin are dashed lines.

microstructural evolution, i.e. in this case assuming that plastic spin vanishes, leads to  $\beta = \beta_0 = \text{constant}$ , which clearly is not observed. Nesterova et al. [31] considered simple shear loading of cold-rolled steel sheets (material B) at various angles to the rolling direction. They also observed significant rotation of the loading axes with respect to the axes of symmetry (using X-ray texture measurements) as seen in Fig. 4; the solid curves are predictions based upon the constitutive model for microstructural evolution and the dashed curves correspond to the vanishing of plastic spin. Other experimental studies of off-axis texture evolution [32–34] all established the fact that the microstructure does not rotate with the material. Similar effects are known for composites [40,41] and polymers [42–44].

**4. Estimates of strain maxima under tensile loadings**

Under tensile loading, a specimen tends to reach a load maximum at the onset of necking. For off-axis loading, rotation of the tensile axis relative to material symmetry planes also plays an important role. A relatively simple, Considere criterion, can be applied to investigate the effects of microstructural evolution on limits to ductility. Consider uniaxial stressing, with

$$\sigma = \sigma_Y(\epsilon_e^p, \beta) = C(\beta)\sigma_e(\epsilon_e^p) \tag{22}$$

As depicted in Fig. 2,  $\beta$  characterizes the orientation of the loading axes relative to the principle axes of anisotropy, which in general varies with deformation. From (22), the condition for load maximum is:

$$dP = d(\sigma A) = \left( \frac{\partial \sigma}{\partial \epsilon_e^p} d\epsilon_e^p + \frac{\partial \sigma}{\partial \beta} d\beta \right) \cdot A + \sigma \cdot dA = 0 \tag{23}$$

where the first term represents material hardening, the second *microstructural hardening or softening* and the third geometric softening. As an example, consider material C of Table 1 which is fit to the data of Kim and Yin [33] and displays trends

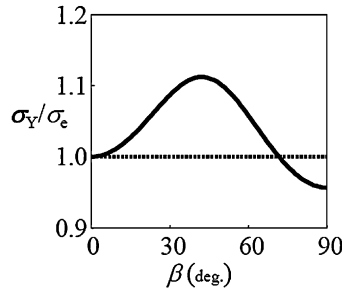


Fig. 5. Normalized uniaxial yield stress versus orientation of the tensile axis  $\beta$  for material C (Kim and Yin [33] data).

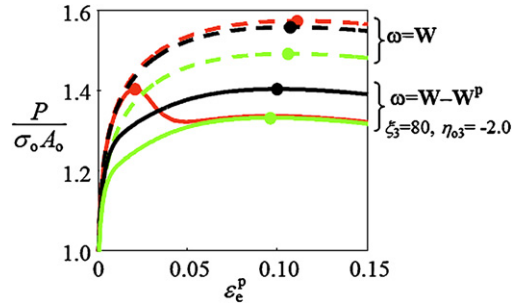


Fig. 6. Nominal uniaxial stress versus strain for  $\beta_0 = 30^\circ$  (red),  $45^\circ$  (green),  $60^\circ$  (black) for material C. Load maxima indicated by filled circles. Dashed curves without effects of microstructural evolution, i.e. for vanishing plastic spin.

similar to the results shown in Fig. 3. Power-law hardening is assumed:  $\sigma/\sigma_0 = (\varepsilon/\varepsilon_0)^N$  with  $N = 0.1$  and  $\varepsilon_0 = 0.001$ . For that material, the variation of the uniaxial yield stress in the plane of the sheet as predicted by the Hill yield criterion (18) is plotted in Fig. 5, which depicts a moderate degree of anisotropy. Load versus plastic strain curves are plotted in Fig. 6 for three initial orientations of the tensile axes relative to the rolling direction. The solid curves are predictions with microstructural evolution, while the dashed curves correspond to  $\beta$  fixed. For all three cases, microstructural evolution significantly lowers the maximum load, and a significant reduction in ductility also is predicted for  $\beta_0 = 30^\circ$ .

## 5. Conclusions

A continuum-level theory for microstructural evolution has been developed for anisotropic materials with locally orthotropic properties. Based upon the conventional elastic–plastic decomposition, constitutive equations for plastic response are expressed in the intermediate configuration where the director vectors (orthotropic axes) have the same orientation as in the initial configuration. The rotation of orthotropic axes is governed by the microstructural spin, which depends on the elastic part of the deformation gradient and, in turn, the partition of the total rotation into elastic and plastic parts. Given that there is freedom in specifying the intermediate configuration, there also is freedom in specifying rotation of the microstructure relative to the material rotation. Constitutive equations for microstructural spin, which is the difference between the material and plastic spins, are defined in terms of the variables in the intermediate configuration, including a generally non-symmetric stress measure that is work-conjugate to the plastic part of deformation gradient. In the case of small elastic strains, that anti-symmetric stress is shown to be relatively small compared with the symmetric stress, but it does contribute to the plastic response.

Representations are developed for scalar- and tensor-valued functions depending on variables in the intermediate configuration, which include a rank-two symmetric tensor associated with orthonormal director vectors and the generally non-symmetric stress. A reduced set of invariants and generators are derived from the components of tensors in the intermediate configuration with respect to the orthotropic symmetry axes. Based on these representations, a key connection is derived between the components of the plastic parts of the rate of stretching and the spin. Plastic spin is shown to be associated with the non-coaxiality between the plastic rate of stretching and the orthotropic axes in the intermediate configuration.

Relations that determine the plastic spin in terms of the plastic part of the rate of stretching have been proposed in terms of six parameters, which for certain symmetries reduce to two. Comparisons with experimental results demonstrate that the constitutive model can represent macroscopic aspects of microstructural evolution of textured polycrystals under simple shear and uniaxial tension, including reverse plastic loading. A significant effect on the maximum load and corresponding strain under uniaxial tensile loading is predicted.

## Acknowledgements

This research was supported by the NSF under Grants No. DMR 02-19243 and CMMI 09-00058 and by DOE/ASCI through Lawrence Livermore National Laboratory.

## References

- [1] Y.F. Dafalias, Corotational rates for kinematic hardening at large plastic deformations, *ASME J. Appl. Mech.* 50 (1983) 561–565.
- [2] Y.F. Dafalias, The plastic spin concept and a simple illustration of its role in finite plastic transformations, *Mech. Mater.* 3 (1984) 223–233.
- [3] Y.F. Dafalias, The plastic spin, *ASME J. Appl. Mech.* 52 (1985) 865–871.
- [4] S. Nemat-Nasser, *Plasticity: A Treatise on Finite Deformation of Heterogeneous Inelastic Materials*, Cambridge University Press, 2004.
- [5] R.J. Asaro, V.A. Lubarda, *Mechanics of Solids and Materials*, Cambridge University Press, 2006.
- [6] M. Berveiller, A. Zaoui, An extension of the self-consistent scheme to plastically flowing polycrystals, *J. Mech. Phys. Solids* 26 (1979) 325–344.
- [7] R. Masson, A. Zaoui, Self-consistent estimates for the rate-dependent elastoplastic behaviour of polycrystalline materials, *J. Mech. Phys. Solids* 47 (1999) 1543–1568.
- [8] M. Bornert, R. Masson, P. Ponte Castaneda, A. Zaoui, Second-order estimates for the effective behaviour of viscoplastic polycrystalline materials, *J. Mech. Phys. Solids* 49 (2001) 2737–2764.
- [9] J. Mandel, *Plasticité classique et viscoplasticité*, Courses and Lectures no. 97, Int. Center for Mech., Springer, Udine, 1971.
- [10] J. Mandel, Equations constitutive et directeurs dans les milieu plastiques et viscoplastiques, *Int. J. Solids Struct.* 9 (1973) 725–740.
- [11] J. Kratochvil, On a finite strain theory of elastic–inelastic materials, *Acta Mech.* 16 (1973) 127–142.
- [12] B. Halphen, Sur le champ des vitesses en thermoplasticité finie, *Int. J. Solids Struct.* 11 (1975) 947–960.
- [13] B. Lorent, On the effects of plastic rotation in the finite deformation of anisotropic elastoplastic materials, *Mech. Mater.* 2 (1983) 287–304.
- [14] E. Van Der Giessen, Continuum models of large deformation plasticity. Part I: Large deformation plasticity and the concept of a natural reference state, *Eur. J. Mech. A Solids* 8 (1989) 15–34.
- [15] E. Van Der Giessen, Micromechanical and thermodynamic aspects of the plastic spin, *Int. J. Plast.* 7 (1991) 365–386.
- [16] Q.S. Zheng, Theory of representations for tensor functions – A unified approach to constitutive equations, *Appl. Mech. Rev.* 47 (1994) 546–587.
- [17] J.P. Boehler, Applications of Tensor Functions in Solid Mechanics, vol. 292, CISM International Centre for Mechanical Sciences, Springer-Verlag, 1987.
- [18] A.C. Eringen, *Mechanics of Continua*, Robert E. Krieger Publishing Company, 1980, Appendix B, pp. 530–536.
- [19] R.J. Asaro, J.R. Rice, Strain localization in ductile single crystals, *J. Mech. Phys. Solids* 25 (1971) 309–338.
- [20] P. Tugcu, K.W. Neale, On the implementation of anisotropic yield functions into finite strain problems of sheet metal forming, *Int. J. Plast.* 15 (1999) 1021–1040.
- [21] Y.F. Dafalias, Orientational evolution of plastic orthotropy in sheet metals, *J. Mech. Phys. Solids* 48 (2000) 2231–2255.
- [22] R. Hill, *The Mathematical Theory of Plasticity*, XII. Plastic Anisotropy, Oxford University Press, Oxford, 1950, pp. 317–334.
- [23] R.S. Rivlin, J.L. Ericksen, Stress–deformation relations for isotropic materials, *J. Rat. Mech. Anal.* 4 (1955) 323–425.
- [24] G.F. Smith, On a fundamental error in two papers of C.C. Wang, *Arch. Rational Mech. Anal.* 36 (1970) 161–165.
- [25] G.F. Smith, On isotropic functions of symmetric tensors, skew-symmetric tensors and vectors, *Int. J. Eng. Sci.* 9 (1971) 899–916.
- [26] C.C. Wang, On the representation for isotropic functions. Part I. Isotropic functions of symmetric tensors and vectors, *Arch. Rational Mech. Anal.* 33 (1969) 249–267.
- [27] C.C. Wang, On the representation for isotropic functions. Part II. Isotropic functions of skew-symmetric tensors, symmetric tensors and vectors, *Arch. Rational Mech. Anal.* 33 (1969) 268–287.
- [28] H. Pan, J.L. Bassani, Microstructural evolution for orthotropic plastic flow, 2011, in preparation.
- [29] J.P. Boehler, S. Koss, Evolution of anisotropy in sheet-steel submitted to off-axes large deformation, in: *Advances in Continuum Mechanics*, Springer, Heidelberg, 1991.
- [30] G. Losilla, J.P. Boehler, Q.S. Zheng, A generally anisotropic hardening model for big offset-strain yield stresses, *Acta Mech.* 144 (2000) 169–183.
- [31] E.V. Nesterova, B. Bacroix, C. Teodosiu, Microstructure and texture evolution under strain-path changes in low-carbon interstitial-free steel, *Metall. Mater. Trans. A* 32 (10) (2001) 2527–2538.
- [32] B. Bacroix, Z. Hu, Texture evolution induced by strain path changes in low carbon steel sheets, *Metall. Mater. Trans. A* 26 (1995) 601–613.
- [33] K.H. Kim, J.J. Yin, Evolution of anisotropy under plane stress, *Int. J. Mech. Phys. Solids* 45 (1997) 841–851.
- [34] H.J. Bunge, I. Nielsen, Experimental determination of plastic spin in polycrystalline materials, *Int. J. Plast.* 13 (1997) 435–446.
- [35] R. Hill, Theoretical plasticity of textured aggregated, *Math. Proc. Cambridge Philos. Soc.* 85 (1979) 179–191.
- [36] R. Hill, Constitutive modeling of orthotropic plasticity in sheet metals, *J. Mech. Phys. Solids* 38 (1990) 405–417.
- [37] J.L. Bassani, Yield characterization of metals with transversely isotropic plastic properties, *Int. J. Mech. Sci.* 19 (1977) 651–660.
- [38] F. Barlat, J. Lian, Plastic behavior and stretchability of sheet metals. Part I: A yield function for orthotropic sheets under plane stress conditions, *Int. J. Plast.* 5 (1989) 51–66.
- [39] G. Ferron, R. Makkouk, J. Morreale, A parametric description of orthotropic plasticity in metal sheets, *Int. J. Plast.* 10 (1994) 431–449.
- [40] J.F. Mulhern, T.G. Rogers, A.J.M. Spencer, A continuum model for fiber-reinforced plastic materials, *Proc. R. Soc. Lond. A* 301 (1967) 473–492.
- [41] N. Aravas, Finite elastoplastic transformations of transversely isotropic metals, *Int. J. Solids Struct.* 29 (1992) 2137–2157.
- [42] E.M. Arruda, M.C. Boyce, Evolution of plastic anisotropy in amorphous polymers during finite straining, *Int. J. Plast.* 9 (1993) 697–720.
- [43] S.D. Batterman, J.L. Bassani, Yielding, anisotropy and deformation processing of polymers, *Polymer Eng. Sci.* 30 (1990) 1281–1287.
- [44] J. Pereda, N. Aravas, J.L. Bassani, Finite deformation of anisotropic polymers, *Mech. Mater.* 15 (1993) 3–20.